

Geometric-Mean Back-Projection for Dense-Array

Imaging of Seismic Sources

Principal Investigator: Gregory C. Beroza

Postdoctoral Associate: Lei Yang

Department of Geophysics, Stanford University

We developed a deep-learning-based seismic denoising algorithm to suppress the strong cultural noise in seismic recordings from urban environments. The algorithm is trained using a waveform data set that combines noise sources from the urban Long Beach dense array and high signal-to-noise ratio earthquake signals extracted from the rural San Jacinto dense array. We apply UrbanDenoiser to denoise the Long Beach dense array data and seismograms recorded by isolated stations from regional seismic network and find that seismic noise levels are strongly suppressed relative to seismic signals, so that the seismic signals can be recovered even from noisy seismic data with signal-to-noise ratio (SNR) around one. The seismic detection/location results based on denoised data preserve earthquake events and exclude large amplitude non-earthquake sources. We perform back-projection imaging on the denoised data, and do not find widespread earthquakes below 20 km, but observe seismicity distributed beneath the surface fault trace of Newport-Inglewood Fault.

Network training

We develop UrbanDenoiser by training a deep neural network with seismic noise from the Long Beach dataset and seismic signals from the San Jacinto dataset. The architecture of the neural network is based on that of the DeepDenoiser algorithm¹. The dataset consists of 90-s windows of seismic waveforms for 80,000 noise samples and 33,751 signal samples. The signal and noise samples are randomly split into training and validation sets. We generate noisy waveforms at different SNR levels by combining the signal training set repeatedly with randomly selected noise samples from the noise training set, and randomly shifting the waveform in the window². The input for the neural network is the 2D time-frequency representation of noisy waveforms determined by Short Time Fourier Transform. Both the real and imaginary parts are input into the neural network so that it is able to learn from the time and phase information. The prediction targets are two masks for recovered signal and noise respectively. We generate seismic waveforms for the validation set with the same procedure and apply them for fine-tuning the hyper-parameters of the network. We test the neural network with the additional seismic data from Long Beach seismic recordings.

We extract noise samples from Long Beach data. These waveforms include various kinds of traffic sources (cars, airplanes, helicopters), vibroseis events and

other unknown activities. We collect seismic recordings from all the receivers in the Long Beach Phase B deployment on Julian days 27 and 48, 2012, and select seismic noise samples from them, because there are fewer earthquakes during these two days in the Quake Template Matching (QTM) catalog³. We segment the data in 90-s-long time series and remove those containing earthquake signals either from known seismic events in the QTM catalog or as determined by the PhaseNet algorithm⁴.

The signal samples are extracted from San Jacinto dataset, which were recorded by another dense array deployed on the active Clark branch of San Jacinto Fault from 2014 May 7 to 2014 June 13⁵. This deployment consists of $\sim 1,108$ geophones that collected high-quality seismic signals from small to medium magnitude local earthquakes. The two deployments used the same sensors with the same instrumental response. We select the labeled signals with a strict condition. We run PhaseNet on the continuous data, and the candidate earthquake signal waveforms are selected based on their coherence across the seismic network. We select only those signal windows with $\text{SNR} > 12$ (defined as the root-mean-square ratio of the seismic energy after and before the first arrival) as the labeled signals. We also include 30,000 seismic signal samples from the North California Seismic Network in the training dataset to increase the predictive power of deep neural network and reduce overfitting.

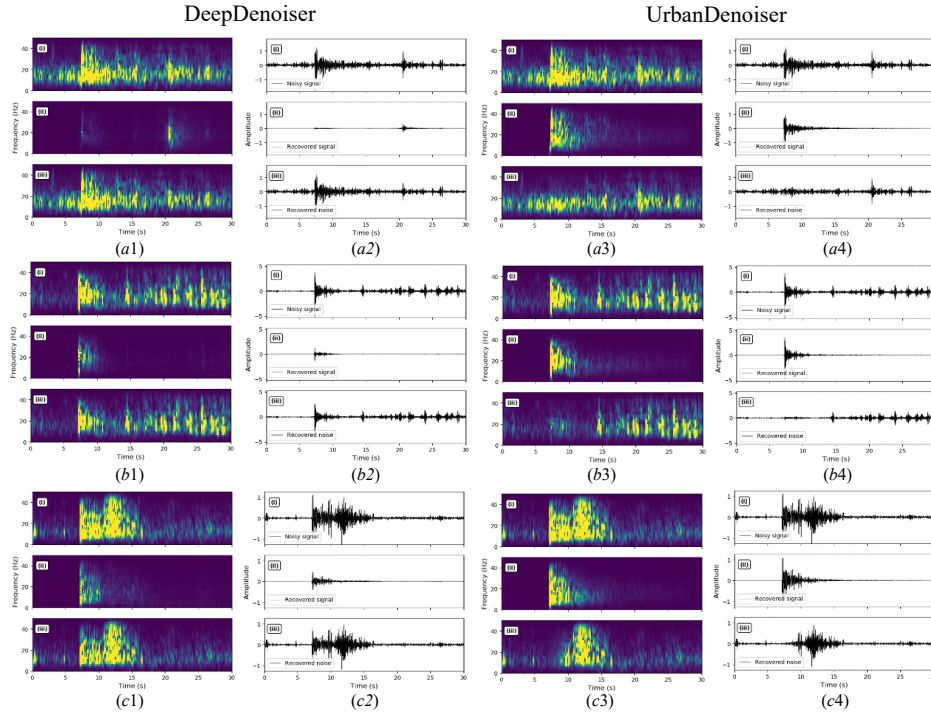


Figure 1: Denoising results on noisy signal windows by DeepDenoiser and UrbanDenoiser. “Noisy signals” in (a1~a4, b1~b4, c1~c4) (i) record a local M 2.1 earthquake. UrbanDenoiser better recovers seismic signals from noisy waveforms compared with DeepDenoiser.

UrbanDenoiser vs DeepDenoiser

We compare the performance of the newly trained UrbanDenoiser and the original DeepDenoiser to the Long Beach data that were not included in the training data set. Figure 1 shows denoising results on seismic recordings for a local M 2.1 earthquake.

Because it is trained on the San Jacinto dataset collected from a similar tectonic setting to the Newport-Inglewood fault zone by the same type of receivers as the Long Beach array, UrbanDenoiser better captures the characteristics of the seismic signals from the Long Beach data and separates them from seismic noise than does the original DeepDenoiser.

Earthquake Detection with Denoised Long Beach Dense Array Data

We perform BP for a 4.4 km (X) \times 6 km (Y) \times 25 km (Z) 3D imaging volume with a grid spacing of 200 m in each dimension. The geographic boundary of the imaging volume is shown as the red dashed rectangle in Fig. 1b. We perform BP as described above. We segment the shifted-and-stacked time series for each grid point into three-second time windows, and the maximum value within each time window is assigned as the BP value of this grid point. We thus obtain a 3D imaging volume for each three-second time window. If the maximum BP value through the whole space within a time window exceeds the detection threshold, we mark the corresponding grid point as a detection.

We apply UrbanDenoiser to seven-days of seismic data (Julian days 61- 67), and perform BP on the denoised continuous data within a 4.4 x 6.0 x 25.0 km³ imaging volume, to detect and locate the most likely seismic sources (Methods). Robust seismic denoising allows us to work on the entire day's data, The denoising effectively removes the daytime/nighttime variation.

Application of UrbanDenoiser to Seismograms from Regional Stations

An earthquake sequence struck urban La Habra with a mainshock magnitude of 5.1 at 4:09:41 UTC on Mar. 29, 2014. We choose the five stations from SCSN nearest to the sequence, and apply UrbanDenoiser to the seismograms. We confirm an earthquake when the detected phases can be associated on two or more stations, and by doing this we find a total of 488 events during the 10 hours between 3:00 ~ 12:00.

Fig. 2 shows 40-minute seismograms (03:20 – 04:00 UTC, Mar. 29, 2014, vertical component only) from the five stations. This is a period between the *M* 3.57 foreshock and *M* 5.1 main shock, and is a relatively quieter window compared with those following the main shock. The only event in the QTM catalog during this time is a *M* 0.67 earthquake at 3:40:59, which is also detected in the denoised waveforms shown in Fig. $a_{4-II} \sim d_{4-II}$. Comparing Fig. $a_{4-II} \sim d_{4-II}$ with the raw data in Fig. $a_{3-II} \sim d_{3-II}$, we find substantial enhancement of the SNR in the denoised version. With the denoised data, we find a total of nine events during this 40-minute period Fig. $a_{4-I} \sim d_{4-I}$, Fig. $a_{4-III} \sim d_{4-III}$ show two examples (not included in QTM catalog) compared with the raw data in Fig. $a_{3-I} \sim d_{3-I}$, Fig. $a_{3-III} \sim d_{3-III}$. This demonstrates that UrbanDenoiser can facilitate the detection of more small events in an urban setting.

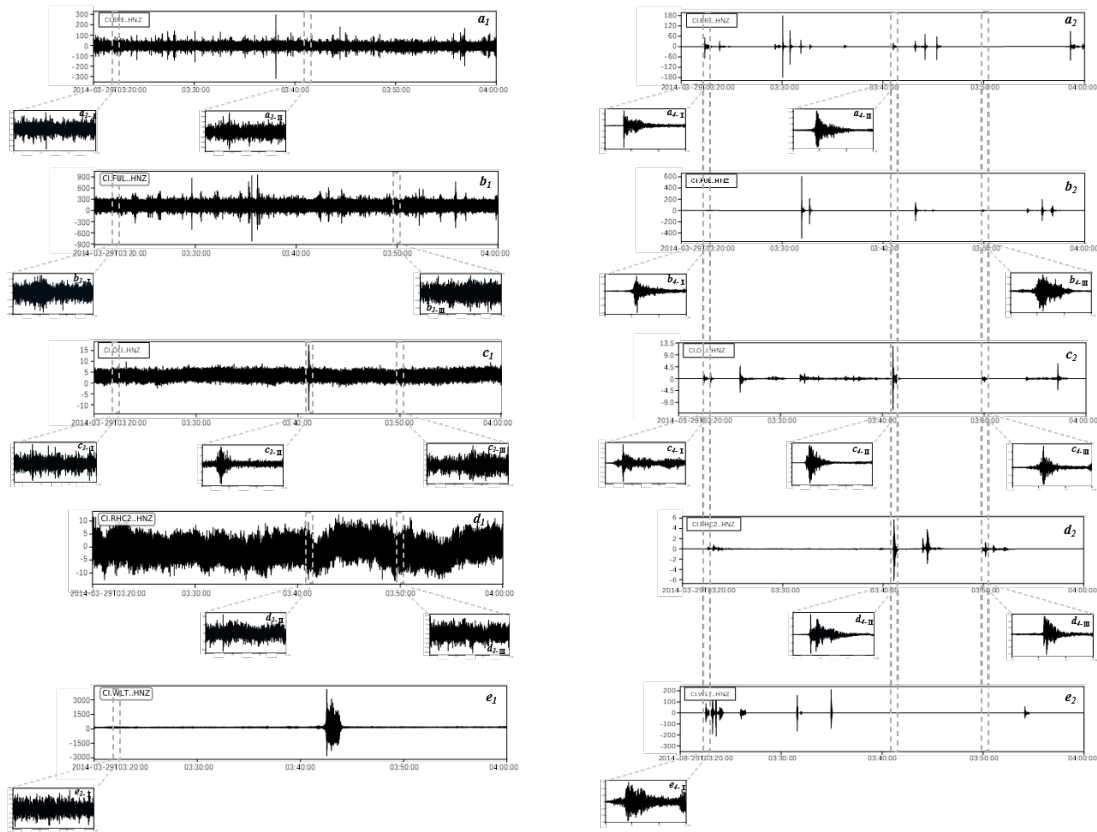


Figure 2: Application of UrbanDenoiser to the 40-minute seismograms (3:20 – 4:00 UTC, Mar. 29, 2014, vertical component) from the five stations of SCSN (Station CI.BRE, CI.FUL, CI.OLI, CI.RHC2 and CI.WLT): (a1-e1) Raw seismograms; (a2-e2) Denoised seismograms; (a4-e4) Zoomed view of the denoised potential earthquake waveforms compared with the raw waveforms (a3-e3).

Fig. 3 compares the SNR of the denoised signals vs. non-denoised signals from Station CI.FUL for 102 events with $-0.16 < M < 5.1$. The SNR of the non-denoised data decreases rapidly with decreasing magnitude (black dots). UrbanDenoiser enhances the SNR for each event (red dots). Although the SNR of the denoised data decreases when the magnitude decreases, the SNR is consistently higher, and the trend is slower. On average, UrbanDenoiser enhances the SNR by about ten-fold, with the most dramatic improvement around M 1.5 - 3.8 (SNR: 2 - 100). This compares with a recently reported increase of ~ 5 dB in SNR reported for more denoising applied to more typical seismological settings⁸.

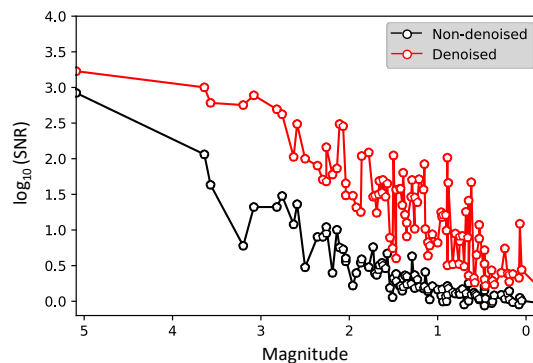


Figure 3: SNR of the denoised signals vs non-denoised signals from Station CI.FUL for 102 events varying between M -0.16 to M 5.1.

Discussion

UrbanDenoiser can effectively suppress the high-level noises, though false positives and false negatives in denoised data should still be expected to occur and need to be assessed. The influence of false positives in denoised data can be effectively suppressed by using the dense array data for detection. False negatives occur when the seismic signal is too weak or when the target seismic phases and the training signal samples are not similar to the earthquake waveforms.

For the most part, we do not have dense array deployments like Long Beach phase A and B available to generate a more complete earthquake catalog. The implementation of seismic monitoring relies on the isolated seismic instrument from the regional seismic network. The conventional STA/LTA method can result in many false detections for phase identification such that it degrades the performance of phase association and event location. UrbanDenoiser can remove most of the noise bursts from the raw data and significantly increase the SNR for the seismic recordings in a single trace. This benefits the subsequent earthquake detection processing, and should enhance the effectiveness of seismic monitoring by regional seismic networks in urban areas.

References.

1. Zhu, W., Mousavi, S. M. & Beroza, G. C. Seismic Signal Denoising and Decomposition Using Deep Neural Networks., *IEEE Trans. Geosci. Remote Sensing* **57**, 9476–9488 (2019).
2. Zhu, W., Mousavi, S. M. & Beroza, G. C. Seismic signal augmentation to improve generalization of deep neural networks, *Advances in Geophysics*, **61**, 151–177 (2020).
3. Ross, Z. E., Trugman, D. T., Hauksson, E. & Shearer, P. M. Searching for hidden earthquakes in Southern California, *Science*, **364**, 767–771 (2019).
4. Zhu, W. & Beroza, G. C. PhaseNet: A Deep-Neural-Network-Based Seismic Arrival Time Picking Method, *Geophys. J. Int.*, **216**, 261–273 (2018).
5. Ben-Zion, Y. *et al.* Basic data features and results from a spatially dense seismic array on the San Jacinto fault zone, *Geophys. J. Int.*, **202**, 370–380 (2015).
6. Inbal, A., Clayton, R. W. & Ampuero, J.-P. Imaging widespread seismicity at midlower crustal depths beneath Long Beach, CA, with a dense seismic array: Evidence for a depth-dependent earthquake size distribution. *Geophys. Res. Lett.* **42**, 6314–6323 (2015).
7. Yang, L., Liu, X. & Beroza, C. G. Revisiting Evidence for Widespread Seismicity in the Upper Mantle under Los Angeles. *Sci. Adv.* **7**, eabf2862 (2021).
8. Tibi, R., Hammond, P., Brogan, R., Young, C. J. & Koper, K. Deep Learning Denoising Applied to Regional Distance Seismic Data in Utah. *Bull. Seismol. Soc. Am.*, **111**, 775–790 (2021).